CCSBT-ESC/2608/BGD 03
(*Previously* CCSBT-OMMP/2606/06)
(ESC Agenda item 7.1)

Update of CPUE abundance index using GAM for southern bluefin tuna in CCSBT (GAM22) up to the 2025 data

CCSBT のミナミマグロについての GAM を用いた CPUE 資源豊度指数（GAM22）の 2025 年データまでの更新

Tomoyuki ITOH and Norio TAKAHASHI
伊藤智幸・高橋紀夫
Fisheries Resources Institute, Japan Fisheries Research Agency
水産研究･教育機構 水産資源研究所

要約

2022 年 ESC27 では、GAM を用いた 2 段階のデルタログノーマルアプローチで CPUE を標準化して面積重みづけする、新たなミナミマグロの CPUE 資源量指数の作成方法に合意した。合意された方法に従った CPUE 資源量指数（GAM22）の作成を、2025 年までの漁獲データに対して実施した。本文書ではベースケースの結果と、様々な感度分析を行った結果を示す。得られた指数値では 2025 年に 2024 年よりも増加し、1969 年からのシリーズでの最高値に達した。モデル選択、レトロスペクティブ解析、対象年齢の変更を含む様々な感度分析に対して資源量指数は頑健であった。

Summary

At ESC27 in 2022, the new calculation for the abundance index of southern bluefin tuna, which was standardized via a generalized additive model in the two-step delta log-normal approach with area weighting, was agreed. The CPUE abundance index (GAM22) was updated for fishery data up to 2025 according to the agreed methodology. This document presents the base case results as well as the results of various sensitivity tests. The index value increased in 2025 from 2024 and reached the highest value since 1969. The abundance index was robust to a variety of sensitivity analyses, including model selection, retrospective analysis, and age range changes.

1. Introduction

Stock assessment and stock management through the Management Procedure (MP) of southern bluefin tuna (*Thunnus maccoyii*; SBT) in CCSBT have historically relied strongly on the abundance index obtained from the CPUE (number of fish / 1000 hooks) of the Japanese commercial longline fishery. In the old days, Nishida and Tsuji (1998) developed a model to calculate the abundance index using the generalized linear model (GLM). Since 2007, an alternative abundance index was developed, which called the core vessel CPUE standardized by GLM in response to the shrinking operating area in time and space and the problem of target fish species (ESC12 report, Itoh et al. 2008). The CPUE abundance index has been used as one of the main abundance indices in the two MPs of the Bali procedure used for the TAC calculation from 2012 to 2020, and the Cape Town Procedure (CTP) used for the TAC calculation since 2021.

It was recognized that the 2018 value of the CPUE abundance index by the core vessel CPUE was anomalously high in ESC24 held in 2019 (ESC24 Report). This prompted further investigation, which subsequently identified that this estimate was generated due to a prediction bias in the GLM standardization method being used, which generated anomalously high estimates for some time-space strata with no fishing effort. At ESC26 in 2021, it was agreed that a new CPUE abundance index should be prepared by May 2022 to assess its impact on MP (ESC26 Report). Through the collaboration work between Japanese scientists and the consultant hired by CCSBT, as well as the discussion and suggestion of the CPUE working group, a new abundance index using CPUE standardized by the generalized additive model (GAM) was developed and agreed at ESC27 in 2022 (OMMP12 and ESC27 Reports). The abundance index is referred to as *GAM22*, because it was agreed in 2022.

This document presents the CPUE results obtained by updating the data to 2025 using the agreed GAM methodology not only for the base case but also for the various sensitivity analyses (Itoh and Takahashi 2022, 2023, 2024, 2025). Furthermore, another paper examines the values predicted by the model for the time-space strata with no effort (Itoh 2026b).

2. Materials and Methods

2-1. Dataset used

The dataset was extracted from logbook data for the Japanese longline fishery, which includes the period from 1969 to the latest year (currently 2025). Following procedures for the conventional SBT CPUE abundance index, records in statistical Areas between 4 and 9 and from April to September were selected. From the logbooks, year, month, latitude (in 1 degree), longitude (in 1 degree), vessel ID (available from 1979), number of hooks used, number of fish caught of SBT, bigeye tuna (*T. obesus*, BET), yellowfin tuna (*T. albacares*, YFT), albacore (*T. alalunga*, ALB) and swordfish (*Xiphias gladius*, SWO) data were used. In the development work in 2022, the number of hooks between floats (HBF; available since 1975) and other fish species (several species of marlines, and butterfly kingfish (*Gasterochisma melampus*; available since 1994)) were examined, and it was decided not to use them so these items were not included in the work this year.

From the size data of the CCSBT database, the age composition of Japanese commercial catch was calculated and converted into the number of fish caught age-4 and older (age-4 plus). The age composition information was first applied to the fork length composition of 50 or more individuals measured in the same month, 5 degrees longitude, and 5 degrees latitude. At this stage, 97% of the number of SBT caught was incorporated and the ratio of age-4 plus was calculated. For records of the conditions for 50 or more individuals were not met the time and space were gradually expanded to correspond to fork length composition, such as the same month - longitude 15 degrees - latitude 5 degrees, the same month -

longitude 15 degrees - latitude 15 degrees, the same quarter - longitude 15 degrees - latitude 5 degrees, the same quarter - Statistical Area (CCSBT Statistical Area), and the same year - Statistical Area, and the same year. The fork length was converted to age by the age-length relationship used by CCSBT. Sensitivity analysis was conducted for age-5 plus and all ages.

The following records were eliminated: hooks 500 or less, hooks 4500 or more, CPUE 200 or higher. As a result of the examination, with the agreement in the CPUE working group discussion in 2022, the record of 50S (50S to 54S), which had a small number of data, were also eliminated.

2-2. Cluster analysis

A cluster analysis was performed to consider the target species of the fishing operations. The *clust_PCA_run* function of the R package *cpue.rfmo* was used. Cluster analysis was performed using the number of fish caught of five species, SBT, BET, YFT, ALB and SWO as data.

2-3. Standardization by GAM

Standardization by GAM was carried out by using the delta log-normal approach. A software for statistical computing and graphics, R (R Core Team 2025) was used for analysis. The *bum* function, which is suitable for large volumes of data, in the *mgcv* package was used. Based on the results of the study by the consultant (Dr. Hoyle), a binomial submodel (hereinafter referred to as BSM) and a positive catch submodel (hereinafter referred to as PCSM) were used, and gamma = 2, binomial distribution and gauss distribution were used, respectively (Hoyle 2022). For the smoother, s (spline) was used for the offset term (hook logarithmic value), and ti (tensor product suitable when there was an interaction with the main effect) was used for the others. cs (cubic regression spline with shrinkage) was used for the basis function (bs) of ti. Gamma is a coefficient multiplied by EDF (described later) and promotes smoothing with values set to >1 (= 1.5 is common).

Binomial submodel

```
cpue > 0 ~ yf +ti(month) + ti(lon) + ti(lat) +
    ti(lon,  lat) + ti(month, lat) + ti(lon, month) + ti(year, lat) + ti(year, lon) + ti(year, month) +
    cl + s(log(hook))
```

Positive catch submodel

```
log(cpue) ~ yf +ti(month) + ti(lon) + ti(lat) +
    ti(lon,  lat) + ti(month, lat) + ti(lon, month) + ti(year, lat) + ti(year, lon) + ti(year, month) +
    ti(lat, month, year) + ti(lat,  lon, month) + ti(lat, lon, year) + ti(year, lon, month) +
    cl + s(log(hook))
```

where,

yf: Year of fishing. In factor.

year: Year. In number

month: Month. In number

lat: Latitude in 5 degree. In number. Represented by the middle (e.g. -47.5 from 45.0S to 49.9S)

lon: Longitude in 5 degrees. In number. Represented by the middle (e.g. 32.5 for 30.0E to 34.9E).

Convert to 360 degree while >240 was converted by -360 so that lon ranged from -22.5 to 187.5 continuously.

cl: Cluster. In factor. 1, 2, 3, and 4.

hook: Number of hooks used. In number.

R code actually used is as follows.

Binomial submodel

```
modA2 <- cpue > 0 ~ yf +
                    ti(month,        k=kA.month11,bs="cs")+
                    ti(lon,          k=kA.lon11,bs="cs")+
                    ti(lat,          k=kA.lat11,bs="cs")+
                    ti(lon,  lat,    k=c(kA.lon21,  kA.lat21), bs="cs")+
                    ti(month, lat,   k=c(kA.month22,kA.lat22), bs="cs")+
                    ti(lon, month,   k=c(kA.lon23,  kA.month23), bs="cs")+
                    ti(year, lat,    k=c(kA.year24, kA.lat24), bs="cs")+
                    ti(year, lon,    k=c(kA.year25, kA.lon25), bs="cs")+
                    ti(year, month,  k=c(kA.year26, kA.month26), bs="cs")+
                    cl+
                    s(log(hook))
mgcv::bam(modA2, data = data, gamma = 2, method = "fREML", family = binomial, discrete=TRUE, nthreads = 10, gc=T)
```

Positive catch submodel

```
modB3 <- log(cpue) ~ yf +
                    ti(month,            k=kB.month11,bs="cs")+
                    ti(lon,              k=kB.lon11,bs="cs")+
                    ti(lat,              k=kB.lat11,bs="cs")+
                    ti(lon,  lat,        k=c(kB.lon21,  kB.lat21), bs="cs")+
                    ti(month,lat,        k=c(kB.month22,kB.lat22), bs="cs")+
                    ti(lon,  month,      k=c(kB.lon23,  kB.month23), bs="cs")+
                    ti(year, lat,        k=c(kB.year24, kB.lat24), bs="cs")+
                    ti(year, lon,        k=c(kB.year25, kB.lon25), bs="cs")+
                    ti(year, month,      k=c(kB.year26, kB.month26), bs="cs")+
                    ti(lat,  month,year, k=c(kB.lat31, kB.month31, kB.year31), bs="cs")+
                    ti(lat,  lon, month, k=c(kB.lat32, kB.lon32, kB.month32), bs="cs")+
                    ti(lat,  lon, year,  k=c(kB.lat33, kB.lon33, kB.year33), bs="cs")+
                    ti(year, lon, month, k=c(kB.year34, kB.lon34, kB.month34), bs="cs")+
                    cl+
                    s(log(hook))
```

mgcv::bam(modB3, data = data.positive, gamma = 2, method = "fREML",family = gaussian, discrete=FALSE, nthreads = 10, chunk.size = 20000, gc=T)

The larger the k value (basis dimension for smoothing flexibility) of the interaction, the better, but the longer the calculation time (Wood, help of *choose.k* in mgcv). The effective degrees of freedom for a model term (EDF) value is calculated by the *k.check* function in the mgcv package, and if EDF was close to k' (the maximum possible EDF for the term), "and" the p-value of k-index is < 0.05, a larger k value was set. The k values were determined by trial and error. Since the k value of the interaction is treated as the value of 2 multiplications (3 multiplications for 3 interactions), it is not necessary to set them separately, however, for the purpose of organizing the work, the k value of each variable in the interaction was set to the same value (i.e. k for year = 20 was used for all interaction terms which include year).

For the diagnosis of the GAM result, the fit was confirmed by the plot diagram (QQ plot, residual distribution) by the *gam.check* function of the mgcv package. AIC was calculated. The distribution of the residuals for each variable was examined. It was examined whether the predicted values were consistent with our knowledge of the distribution of SBT and the plausible trend of SBT stock abundance. We made a comprehensive judgment by looking at this information as well as AIC.

Calculation is performed by a desktop PC (CPU = Intel (R) Core (TM) i9-10900T CPU @ 1.90GHz and 1.90 GHz, RAM = 64.0GB, 64 bit, Windows 11 Pro). The software R (R4.5.2) was used to make the dataset and calculate GAM.

Compared to the work in 2025, in 2026 we sped up calculations by using parallel processing with the bam function using nthreads = 10. Also, instead of using Microsoft R Open 4.0.2, which is no longer supported by the company, we performed GAM standardization using R 4.5.2. We used discrete=T/F in the bam function. The bam manual describes it as follows: *An alternative fitting approach (Wood et al. 2017, Li and Wood, 2019) is provided by the discrete==TRUE method. In this case a method based on discretization of covariate values and C code level parallelization (controlled by the nthreads argument instead of the cluster argument) is used.* For the binomial submodel, we used discrete=TRUE. For the positive catch submodel, although we used discrete=FALSE for the base case, the base case used for sensitivity analysis was the one obtained with discrete=TRUE. This is because the run time for the positive catch submodel was approximately 15 minutes with discrete=TRUE, compared to more than 2 hours with discrete=FALSE. In sensitivity analysis, where numerous runs were performed, shorter runs were more practical.

2-4. Calculation of abundance index

After creating data with all combinations of year / month / latitude / longitude (using R's *expand.grid* function), we made a dummy data set limited to the month / latitude / longitude where the fishing was operated in the past. The predicted value was calculated for each submodel for the dummy data set, and the product of estimates from the two submodels (BSM and PCSM) was calculated. Since the expected value is biased when the log-normal distribution is restored, the predicted value was corrected by adding mean squared error (MSE) / 2 in the case of the positive catch submodel.

Furthermore, the area weighting coefficient was calculated in consideration of the fact that the distance of 1 degree of longitude differs depending on the latitude and the number of 1 degree squares that SBT have been caught in the past within the 5 degree x 5 degree squares. The abundance index can be calculated by the following formula.

Σ(predicted value of binomial submodel of dummy data set × predicted value of positive catch submodel of dummy data set × Area weighting coefficient) / Overall average value.

2-5. Sensitivity analysis

Various sensitivity analyses were performed along the way in selecting the datasets and methods. The same sets of sensitivity analyses performed at the final stage in 2022 were repeated in 2023 and 2024. We omitted some of the analyses where no substantial difference was observed.

Model selection: In some cases, estimation did not converge, and in some cases, even if the AIC was low, the abundance index behaved significantly differently from the others, so a simple selection by AIC seemed inappropriate. For the binomial submodel, we tried the case where all the interactions were removed from the base case, the case where the two-way interaction was removed one by one, and the case where the three-way interaction was added one by one. For the positive catch submodel, we tried the case where all the interactions were removed from the base case, the case where the two-way interaction was removed one by one, and the case where the three-way interaction was removed one by one.

Retrospective analysis: Excludes data from the last year up to the past 10 years. Mohn's rho was calculated as an index of retrospective bias (Hurtado-Ferro et al. 2015).

Selection of k: Effect when k was increased by one step.

Effect of changing age: Age-4 plus used in the base case, but limited to age-5 plus, or all ages were tried.

3. Results

3-1. Dataset used

Data from 1969 to 2025 amounted to 811,642 records. Of these, 715,383 records included a catch of SBT age-4 plus, accounting for 88% of the total. A very high positive catch rate is characteristic of this dataset. By year, the positive catch rate dropped to about 60% in the mid-1990s and around 2010, but otherwise remained above 80% (Fig. 1). The percentage was high in 2025 as well as 2024, and no low values were observed in the aggregated month and 5-degree data (Fig. 1, center panel). The nominal CPUE of the positive catch dataset is high in the 1970s, low in the 1980s to 2000s, and high after 2010. The nominal CPUE in 2025 was the highest in the past 40 years.

Similar figures are shown for other variables, including month, longitude, latitude, and latitude and longitude maps (Fig. 2 and Fig. 3). There is no strong tendency for the month and longitude. For latitude, positive rate and CPUE in the positive catch data were low at 30S, high up to 35S (CPUE) or 40S (positive rate), and 45S was similar to 40S. Data of 30S exists only in the Pacific Ocean (Area 4 and Area 5).

3-2. Cluster analysis

The data were divided into four cluster groups. Relevant figures are shown in Fig. 4 to Fig. 8. Since the eigenvalues are greatly reduced to 2 groups and the decrease to 4 groups is not so large, it may be appropriate to divide them into 2 groups. However, in the analysis of the data up to 2020, there was a problem that the BSM of GAM did not converge when divided into two groups (the data up to 2021 converged in a short time). Therefore, we decided to analyze in 4 groups. Note that the case of 2 groups was carried out by sensitivity analysis in previous years.

The fish species included five species: SBT, BET, YFT, ALB and SWO. At the stage of trial and error in the 2022 work, we also tried 3 species (SBT, BET and YFT) and obtained similar results as 5 species. But 3 species are few and cover all species that can be the main target of operation, it was decided by the CPUE working group to have 5 species (Itoh and Takahashi 2022).

The significant difference was observed among the four clusters in latitude (Fig. 7), however, there

were no noticeable trends in year, month, longitude, number of hooks used, or hooks between floats (HBF). It was probable that HBF had a narrow range in the dataset and did not make a difference because it contained little data of deep longline targeting on BET. Such an effect may have been seen in the waters north of Area 4-9. The main catch in the first cluster, which is located in the southernmost part, was SBT. SBT and ALB were caught in the second cluster. The third cluster was a mixture of SBT and ALB, and the fourth cluster was a mixture of five species.

3-3. Standardization by GAM

For the binomial submodel, the model including all main effects and two-way interaction terms was selected mainly from AIC in the 2022 work. There was a problem that the run did not converge when the three-way interaction term was included. For the positive catch submodel, the model including the main effect and all the two-way and three-way interaction terms was selected mainly from AIC. It was agreed in the ESC in 2022 that these models were used for the base case.

The k value was examined independently for each submodel. The same sets of k used in the 2022 work were utilized (Table 1). Table 2 shows relevant statistics including the EDF value for k and the p value for k-index. There was no term that EDF value close to k' "and" p-value < 0.05.

The diagnosis results are shown in Table 3, Fig. 9, and Fig. 10. The binomial submodel explained 73.8% deviance, and the positive catch submodel explained 49.8%. For BSM, the QQ plot is generally good, although some parts do not fit at both ends. The residual histogram has a single peak and is skewed to near 0 residual. For PCSM, the QQ plot is generally good, and the residuals have a single peak. In the plot of the fit value and the response variable, there is a roughly upward-sloping relationship. Both are judged to be not bad fit.

The residuals were further examined. Plots were made for year, month, latitude, and longitude (Figs. 11 and 12). Note that these figures are not from *gamVis*, which uses simulation. There was too much data and *gamVis* caused a memory over and so we couldn't get any results. These are simple box plots of residuals. For BSM, the median residuals were positively biased in 2004-2007 in the year. There was a slight positive bias for the month. At latitude, the negative bias was large at 30S, a slight positive bias was seen at 35S, and the bias was small at 40S and 45S. At the western end of the longitude, there was a large negative bias.

For PCSM, the bias was small by year and month. At latitude, the range was large at 30S. The bias of the longitude was small, but a negative bias was seen only at the eastern end. When made into a map, the area with zero residuals was greatly expanded in both submodels (Fig. 13). In some places, large residuals may occur in the peripheral waters. It has been confirmed in the 2022 work that the data in the area where these large residuals are seen has a negligible impact on the abundance index.

Box plots of predicted values for variables (year, month, latitude, longitude, latitude x longitude) in the dummy dataset are shown (Fig. 14, Fig. 15, Fig. 16, Fig. 17, and Fig. 18). No inconsistency was found in comparison with the current knowledge of the distribution of SBT and changes in the abundance. The high predicted values in the southeastern waters of Australia (35S, 140E) are interesting (Fig. 18). Currently, there is no fishing operation in this area, but it was confirmed in the 2022 work that fishing was operated in this area in the 1970s and 1980s.

3-4. Calculation of abundance index GAM22

The predicted value of the dummy data set was weighted by the area factor and normalized by the average value to obtain the abundance index as GAM22. To see the effect of area weighting, we compared it with a simple unweighted average (Fig. 19). As a result, it was found that they are similar to each other, and the influence of weighting is small. Since this method includes the interaction of years in the model,

it is no longer necessary to obtain the conventional Constant / Variable square hypothesis and its intermediate index (see Hoyle (2022) for details).

Figure 20 shows the obtained abundance index of GAM22. The values are shown in Table 4. It increased in many years from 2006 to 2025. In 2025, it is the highest value since 1969.

3-5. Sensitivity analysis

Approximation

The bam function manual states that discrete=TRUE will often produce identical results (with discrete=F). However, when using discrete=T and discrete=F with the bam function, while the results were generally similar, differences arose in the abundance index for 2025, with discrete=T resulting in a lower value (Fig. 21).

Model selection

For BSM, a model (modA2) containing all two-way interactions was selected as the base case in the 2022 work. Its AIC was lower than any other model with one term removed from modA2 (Table 5). On the contrary, in the model to which one three-way interaction term was added (e.g. modA2.p14), the AIC was low, but there was a problem that it did not converge sometimes. The difference on the abundance index was small in the models (Fig. 22 and Fig. 23). Therefore, it is considered appropriate to use modA2 as the base case again this year.

For PCSM, a model (modB3) containing all the two-way and three-way interaction terms was selected as the base case in the 2022 work. Its AIC was lower than any other model with one term removed from modB3, except modB3.no6 and modB3.no7 (Table 6). The modB3 was used as the base case again this year. The difference between the models in the abundance index is small (Fig. 24 and Fig. 25). Little differences were seen in modB3.no6 and mdB3.no7. Among these cases, modB3.no9 and mdB3.no14, which exclude ti(year, longitude) and ti(year, longitude, month) respectively, showed a relatively large difference, but the difference was slight.

Retrospective analysis

Figure 26 shows the results of a retrospective analysis of the base case model. Figure 27 shows the results by each submodel. Differences were small in previous years. Mohn's rho was 0.09, less than the +0.20 that indicates caution (Hurtado-Ferro et al. 2015). Note that the last year’s value (2024) was decreased substantially in the updated index, which was caused by the binary submodel.

Selection of k

For BSM, we examined the effect of adding +1 to k of the month, +5 to k of the year, and +5 to k of the longitude. The latitude has already reached the maximum value (k = 4). For PCSM, we examined the effect of increasing the year k by +5 and the longitude k by +5. The month and latitude are already at their maximum.

As a result, there was very little effect on BSM (Fig. 28 and Fig. 29), however, there is some change when kA.year25 (ti(year, lon)) was changed from 10 to 15. It is suggested that k was large enough for most cases. For PCSM, there was a noticeable change when kB.year34 (ti (year, lon, month)) or kB.year31 (ti (lat, month, year)) was changed from 20 to 25 (Fig. 30, Fig. 31). It might be better to consider increasing these k-values associated with year in the future.

Effect of changing age range

The results are shown for the base case of age-4 plus, limited to age-5 plus (Fig. 32), and for all ages (Fig. 33). At age-5 plus, the overall trajectory was similar to the base case up to 2024, but significantly lower in 2025 values. For all ages, the values for 1990-1994 and 2017-2023 were slightly higher, but those in 2024 and 2025 were much higher.

This sensitivity analysis is related to cohort strength. A lower value in age-5 plus would suggest a stronger age-4 cohort in 2025 than in other years. Higher values in 2024 and 2025 in the all-ages would suggest stronger age-3 cohorts in these years. In addition, it also relates to release and discard in the longline operation. When fish is released and discarded from longline vessels, it is often a small fish, age-3 or age-4. The proportion of released fish will depend on the vessel's IQ utilization strategy. If the proportion of released fish changes in a certain year in the future, the effect can be examined by calculating the abundance index for those ages other than 4 and comparing it with the abundance index for those age-4 plus. The proportion of the number of fish released from Japanese longliners has been monitored and calculated as 3.7% of the total catch of age 4 plus on average (Itoh 2026b).

4. Discussion

The 2025 fishing data was added to the dataset. The method using GAM agreed at the 2022 ESC was able to obtain a convergent solution without changing the settings such as the k parameter to the updated dataset. The distribution of the residuals for each variable and the overall fitting of the residuals in the base case were the same as in the previous work, and no problems were observed. The results of the sensitivity analysis were similar to workes have been done since 2022. We have not found any problems using GAM22 for the stock assessment.

5. References

CCSBT (2007) Report of the Twelfth Meeting of the Scientific Committee. 10 - 14 September 2007. Hobart, Australia. 80pp.

CCSBT (2019) Report of the Twenty Fourth Meeting of the Scientific Committee. 7 September 2019. Cape Town, South Africa. 121pp.

CCSBT (2021) Report of the Twenty Sixth Meeting of the Scientific Committee. 31 August 2021. Online. 93pp.

CCSBT (2022a) Report of the Twelfth Operating Model and Management Procedure Technical Meeting. 20-24 June 2022. Hobart, Australia and Online. 33pp.

CCSBT (2022b) Report of the Twenty Seventh Meeting of the Scientific Committee. 29 August-5 September 2022. Online. 114pp.

Hoyle, S. (2022) Validating CPUE model improvements for the primary index of southern bluefin tuna abundance. CCSBT-OMMP/2206/04.

Hurtado-Ferro, F., Szuwalski, C.S., Valero, J.L., Anderson, S.C., Cunningham, C.J., Johnson, K.F., Licandeo, R., McGilliard, C.R., Monnahan, C.C., Muradian, M.L., Ono, K., Vert-Pre, K.A., Whitten, A.R., Punt, A.E., (2015) Looking in the rear-view mirror: bias and retrospective patterns in integrated, age-structured stock assessment models. ICES J. Mar. Sci. 99–110.

Itoh, T., E. Lawrence, and J. G. Pope (2008) The development of new agreed CPUE series for use in future MP work. CCSBT-ESC/0809/09.

Itoh, T. and N. Takahashi (2022) Development of the new CPUE abundance index using GAM for southern bluefin tuna in CCSBT. CCSBT-OMMP/2206/08.

Itoh, T. and N. Takahashi (2023) Update of CPUE abundance index using GAM for southern bluefin tuna in CCSBT up to the 2022 data. CCSBT-OMMP/2306/05

Itoh, T. and N. Takahashi (2024) Update of PUE abundance index using GAM for southern bluefin tuna in CCSBT up to the 2023 data. CCSBT-ESC/2409/21.

Itoh, T. and N. Takahashi (2025) Update of CPUE abundance index using GAM for southern bluefin tuna in CCSBT (GAM22) up to the 2024 data. CCSBT-OMMP/2507/06.

Itoh, T. (2026a) Proposal of a method for checking abundance indices of southern bluefin tuna obtained from longline CPUE. CCSBT-OMMP/2606/07.

Itoh, T. (2026b) Change in operation pattern of Japanese southern bluefin tuna longliners in the 2025 fishing season. CCSBT-OMMP/2606/05.

Nishida T. and S. Tsuji (1998) Estimation of abundance indices of southern bluefin tuna (*Thunnus maccoyii*) based on the coarse scale Japanese longline fisheries data (1969-97). CCSBT/SC/9807/13.

R Core Team (2025) R: A Language and Environment for Statistical Computing. R Foundation for Statistical Computing, Vienna, Austria. <https://www.R-project.org/>.

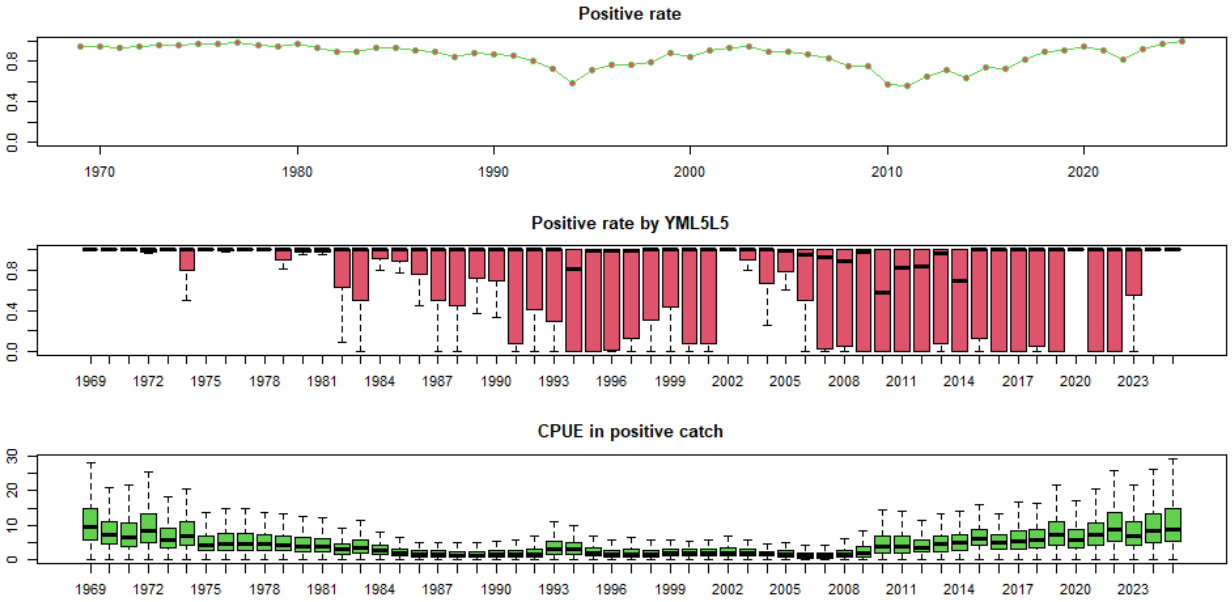


Fig. 1. Nominal value of positive catch rate and CPUE by year.
Upper panel is the positive rate which is the total number of positive catch operations / the total number of all records. Middle panels is boxplot based on the positive catch rate by year, month, 5 degree latitude and 5 degree longitude. Lower panel is CPUE in positive catch records.

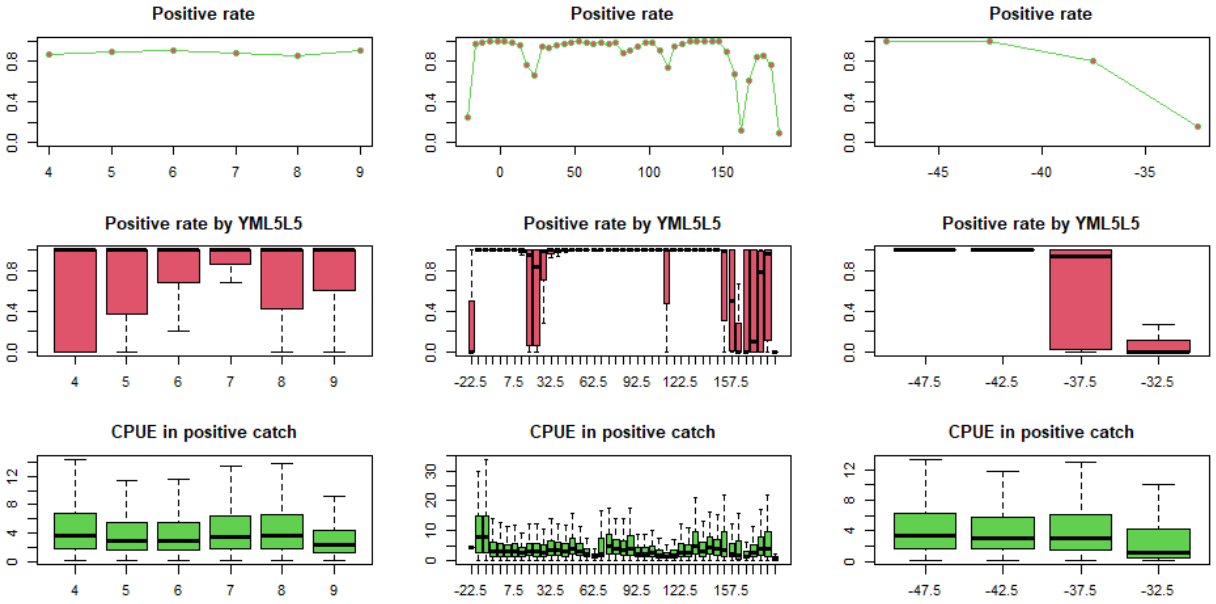


Fig. 2. Nominal value of positive catch rate and CPUE by month, longitude and latitude.
Upper panels are the positive rate which is the total number of positive catch operations / the total number of all records. Middle panels are boxplot based on the positive catch rate by year, month, 5 degree latitude and 5 degree longitude. Lower panels are CPUE in positive catch records.

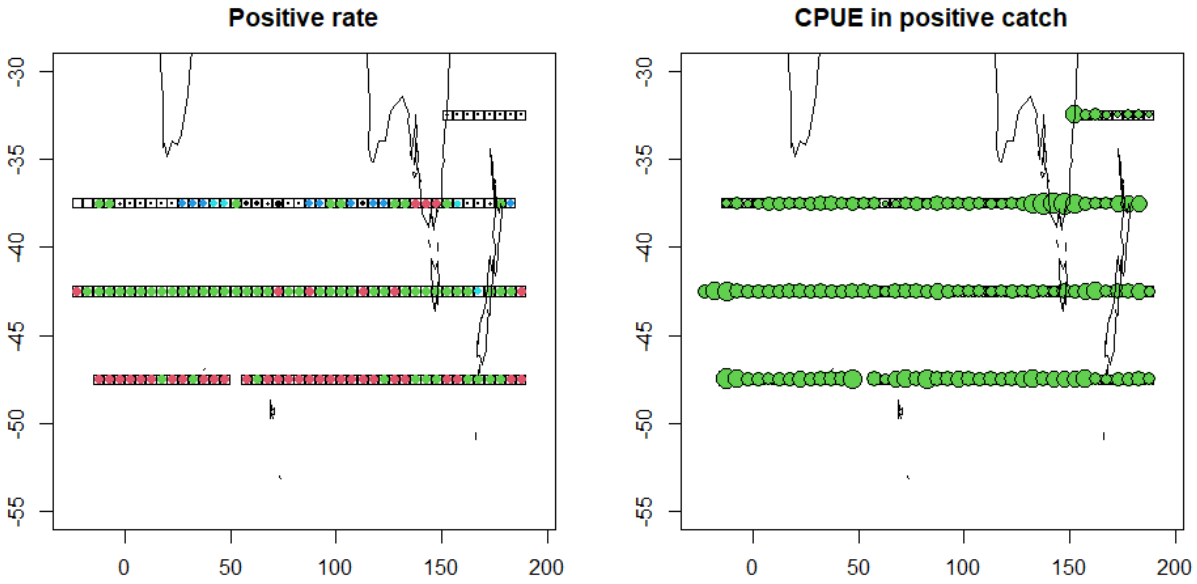


Fig. 3. Nominal value of positive catch rate and CPUE in map.
Left panel is the positive rate. Right panel is CPUE in positive catch records. Red is the higher value, followed by green, blue and white in the positive catch rate panel.

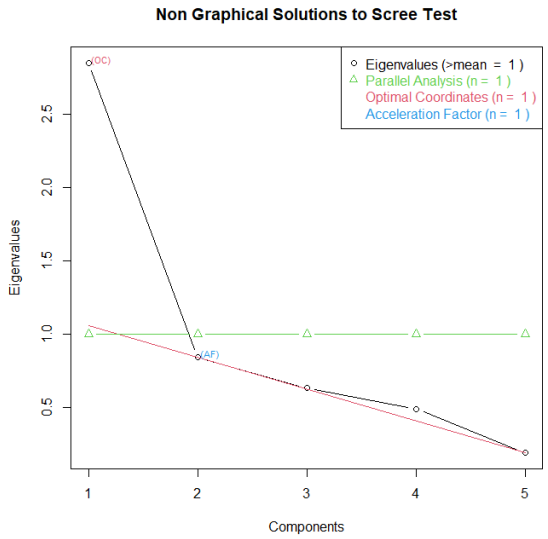


Fig. 4. Eigen values for the number of components in cluster analysis.

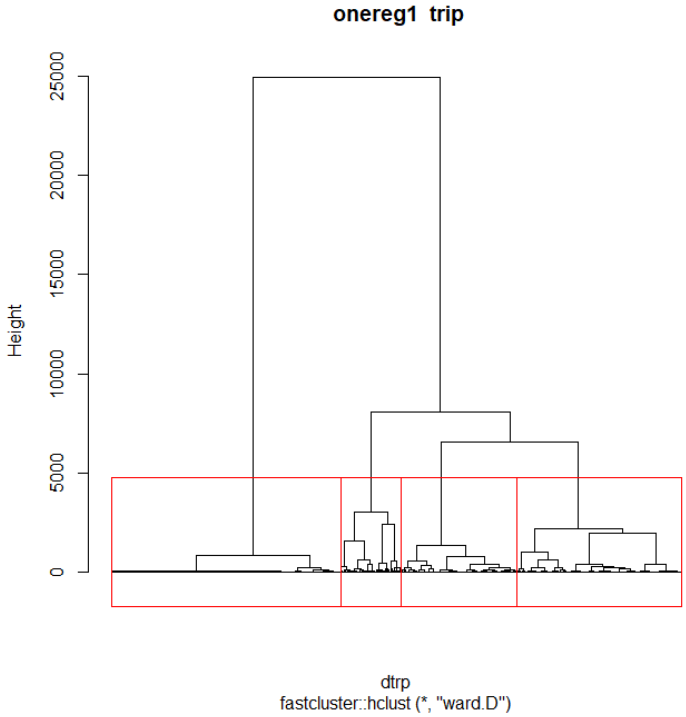


Fig. 5. Dendrogram of the cluster analysis.

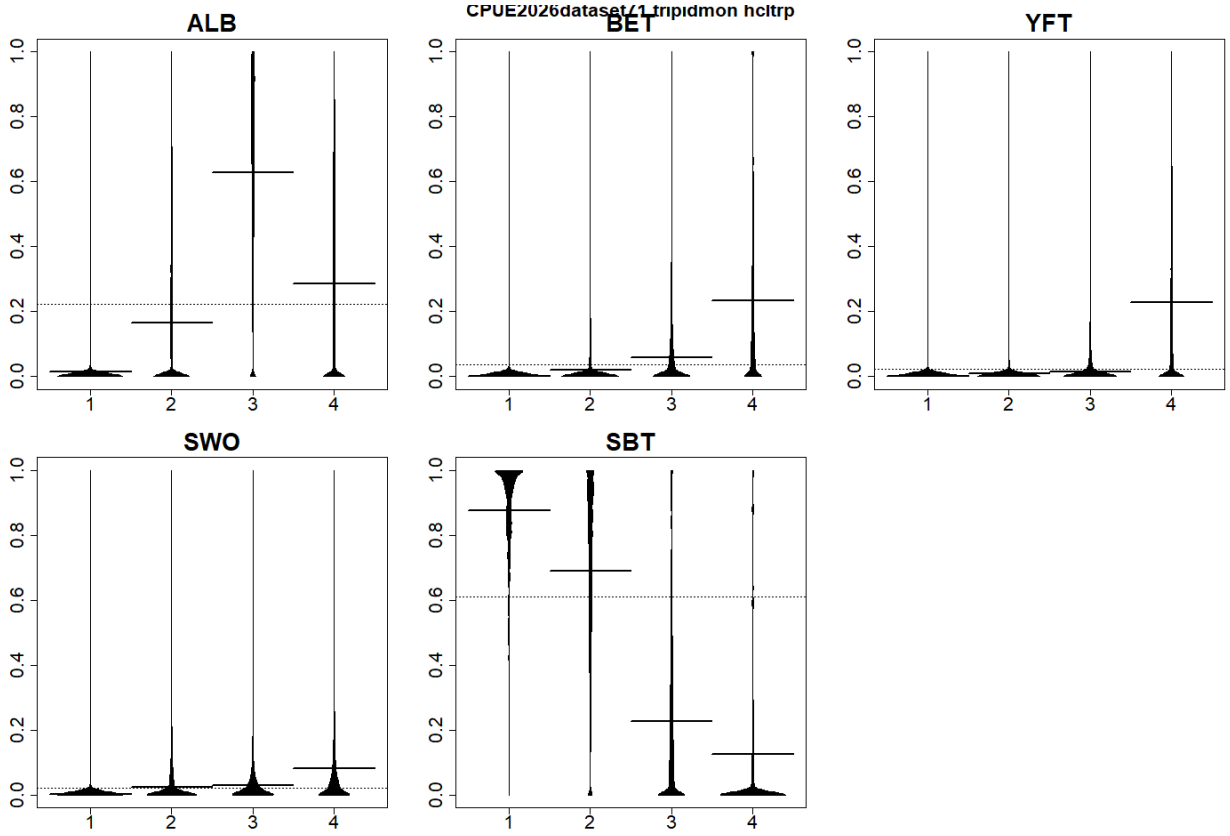


Fig. 6. Occurrence by species in each group in cluster analysis.
ALB is albacore, BET is bigeye tuna, YFT is yellowfin tuna, SWO is swordfish and SBT is southern bluefin tuna.

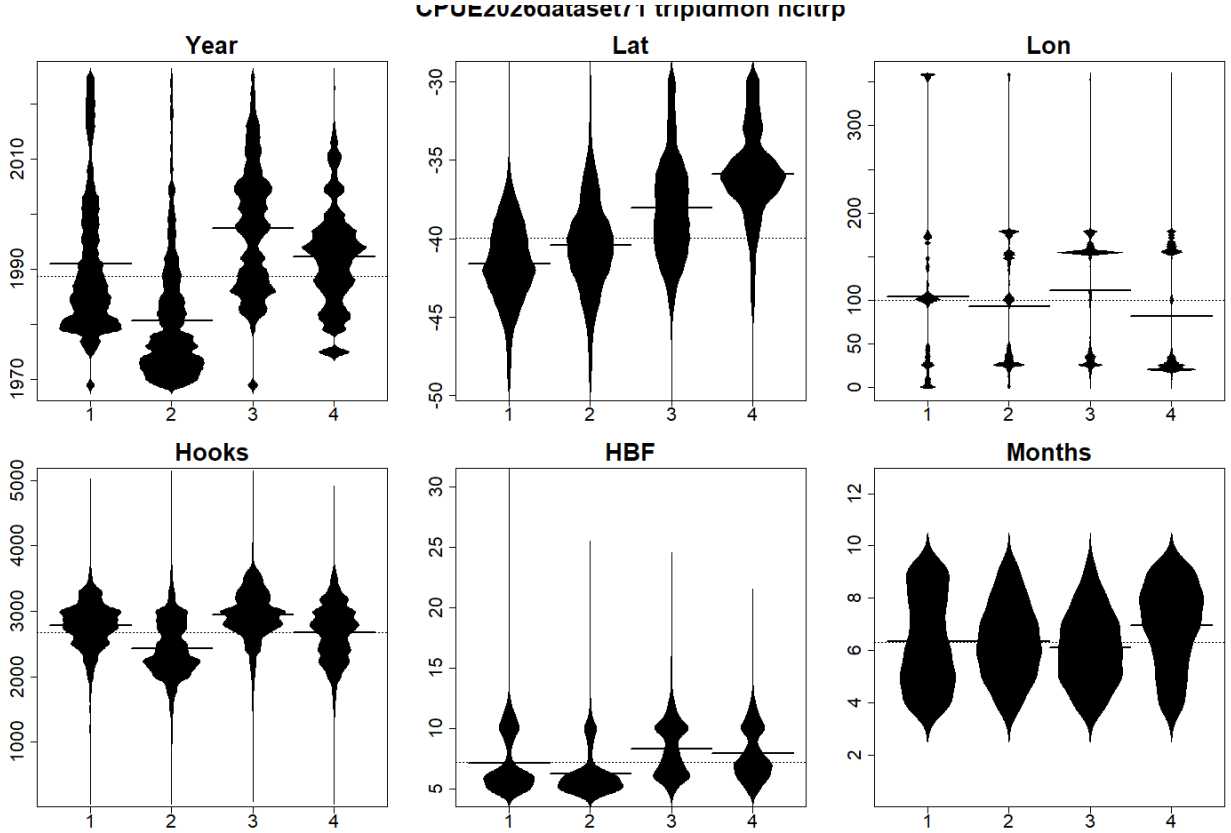


Fig. 7. Occurrence by variables of each group in the cluster analysis.

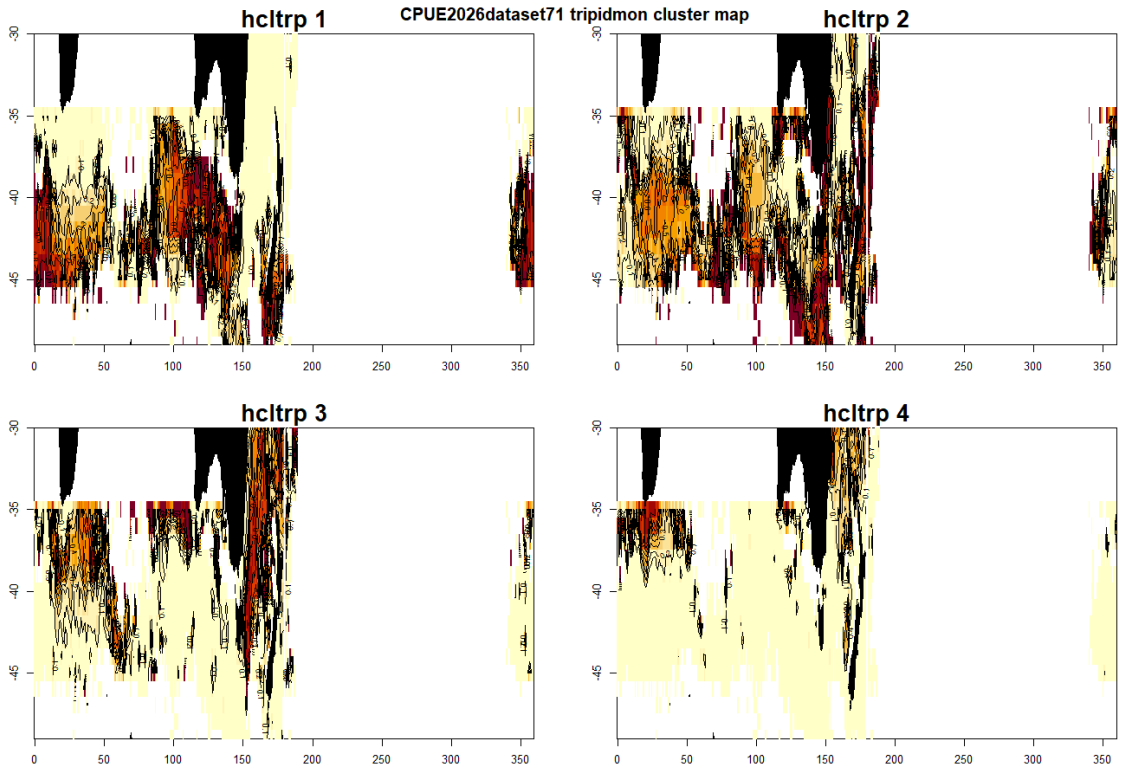


Fig. 8. Occurrence on map by group in the cluster analysis.

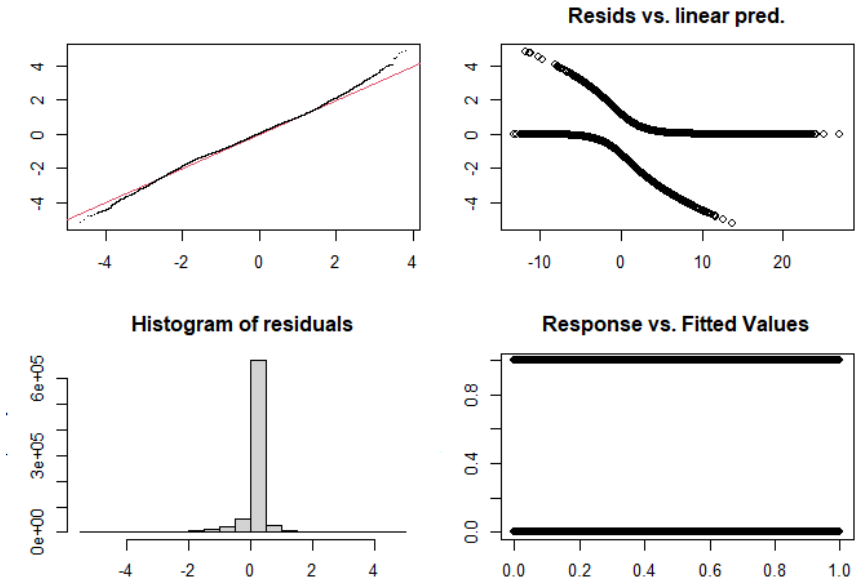


Fig. 9. Diagnostic plots for the binomial sub-model in the base case run.

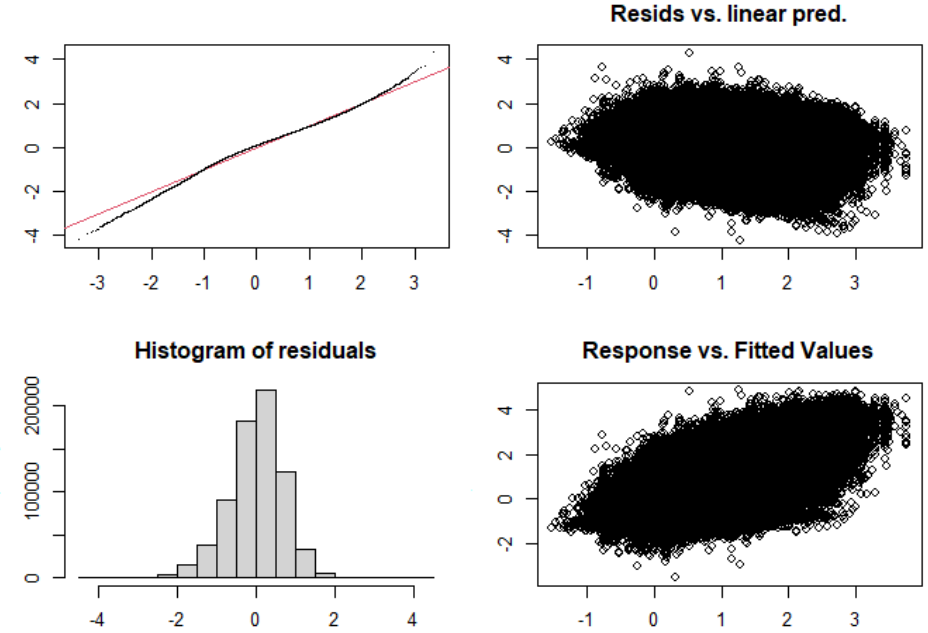


Fig. 10. Diagnostic plots for the positive catch sub-model in the base case run.

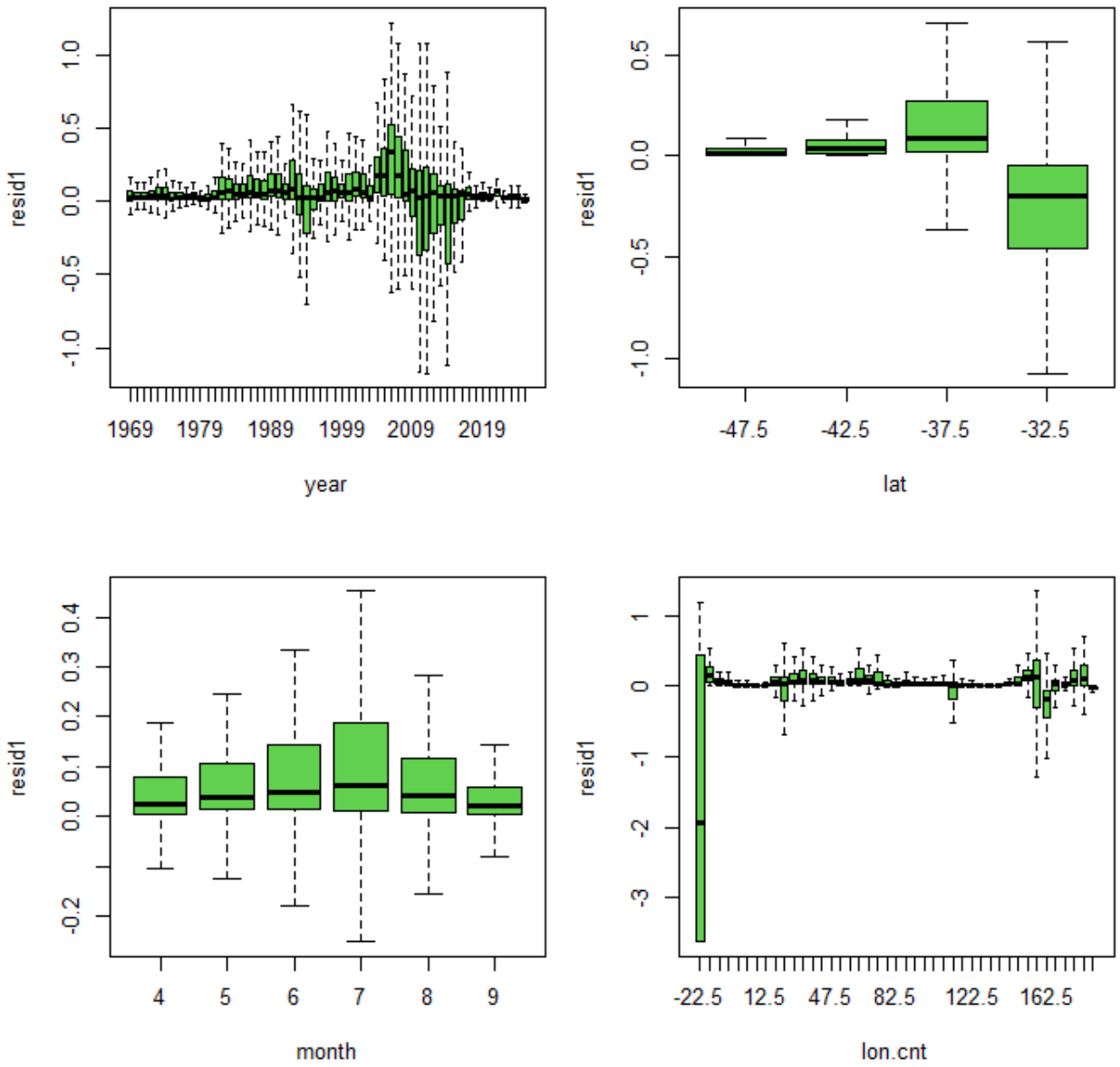


Fig. 11. Residuals by variable in the binomial sub-model in the base case run.

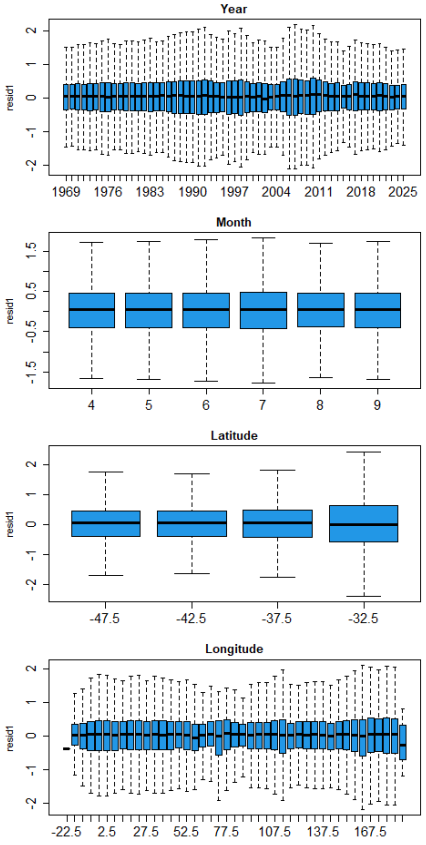


Fig. 12. Residuals by variable in the positive catch sub-model in the base case run.

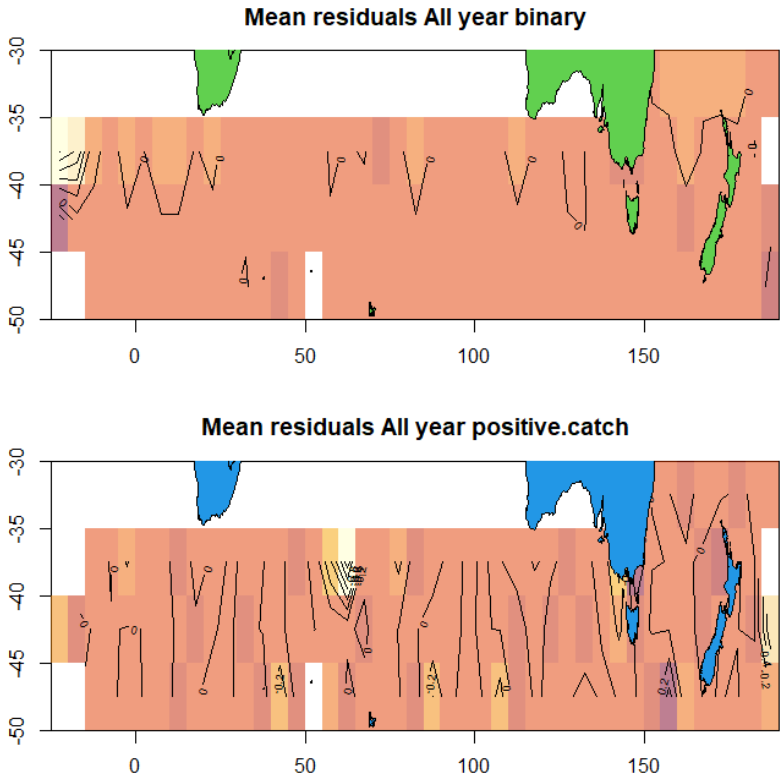


Fig. 13. Residual on maps for both sub-models in the base case run.

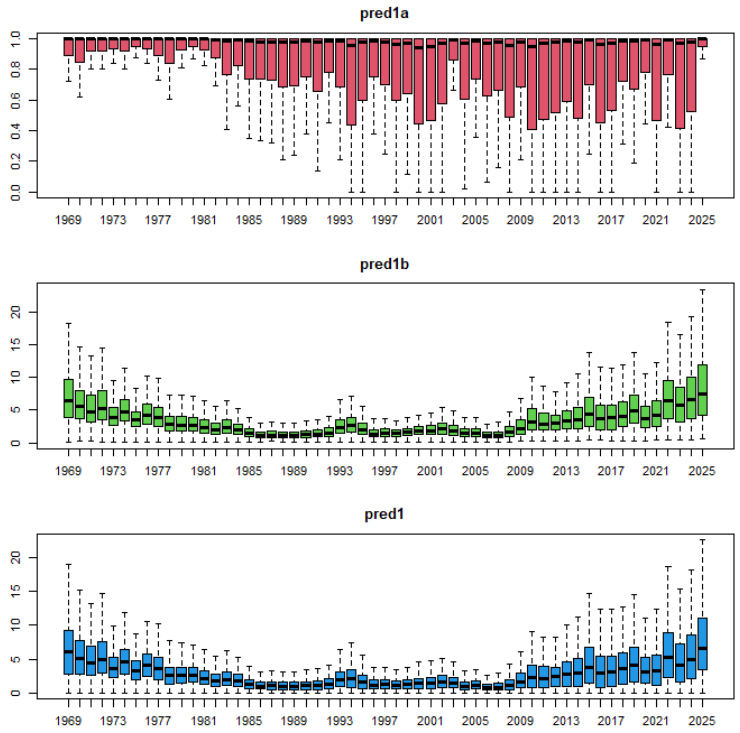


Fig. 14. Predicted value by year in the base case run.

Upper panel is the positive rate obtained from the binomial sub-model. Middle panel is CPUE obtained from the positive catch sub-model. Lower panel is the product of the two.

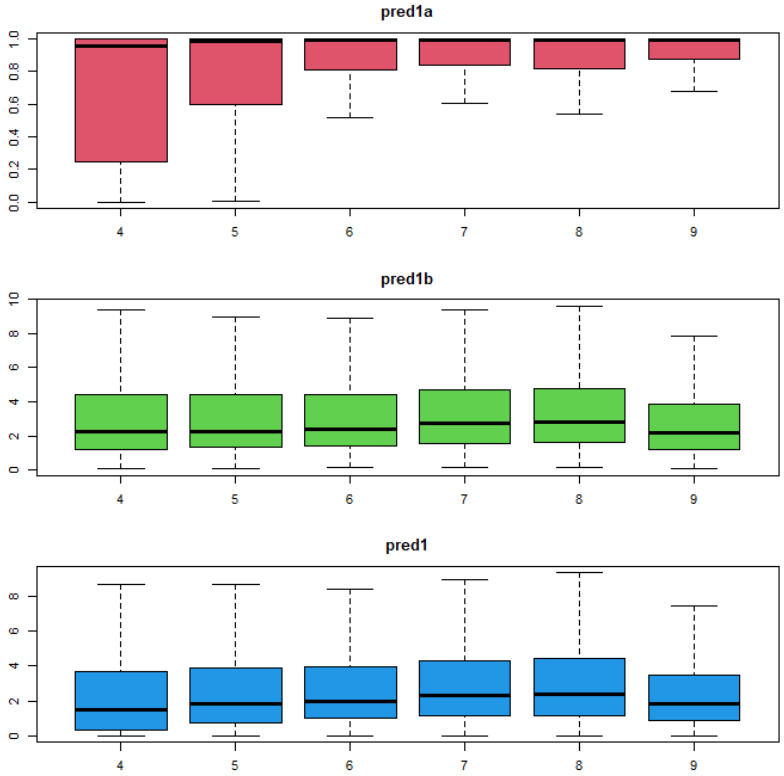


Fig. 15. Predicted value by month in the base case run.

See Fig. 14.

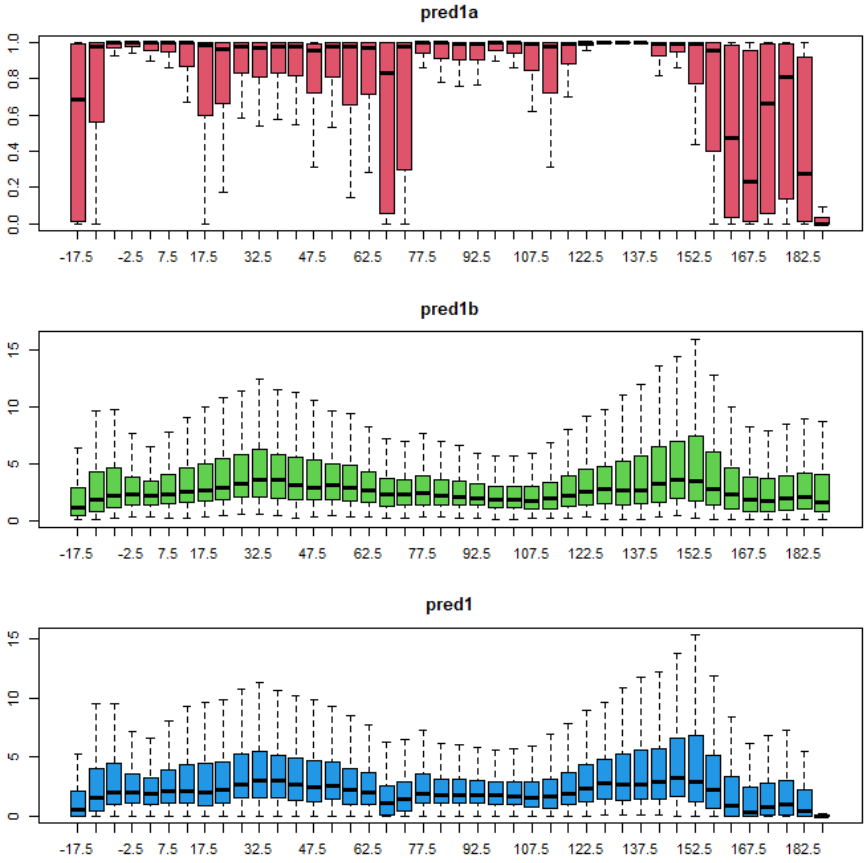


Fig. 16. Predicted value by longitude in the base case run.
See Fig. 14.

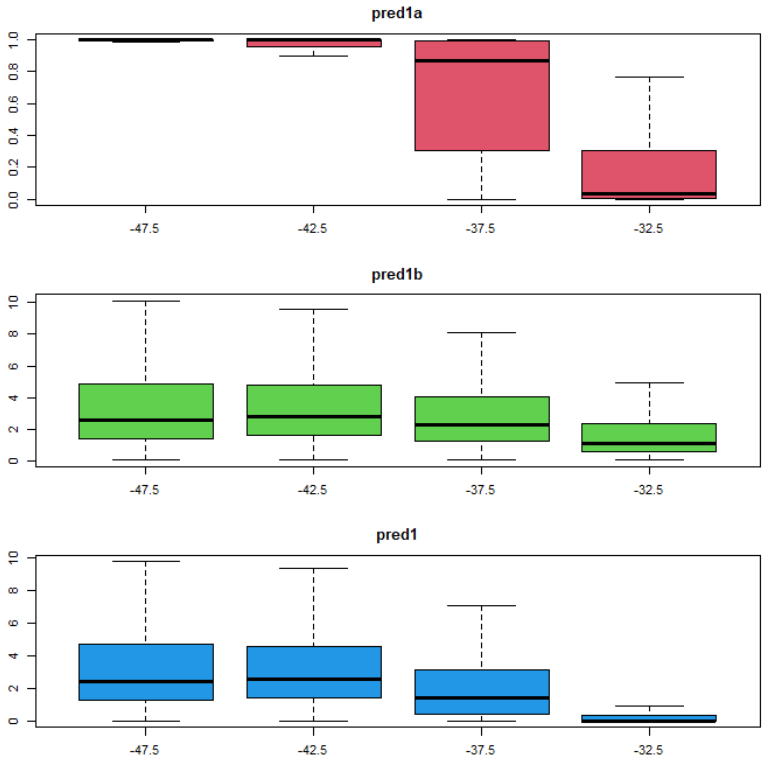


Fig. 17. Predicted value by latitude in the base case run.
See Fig. 14.

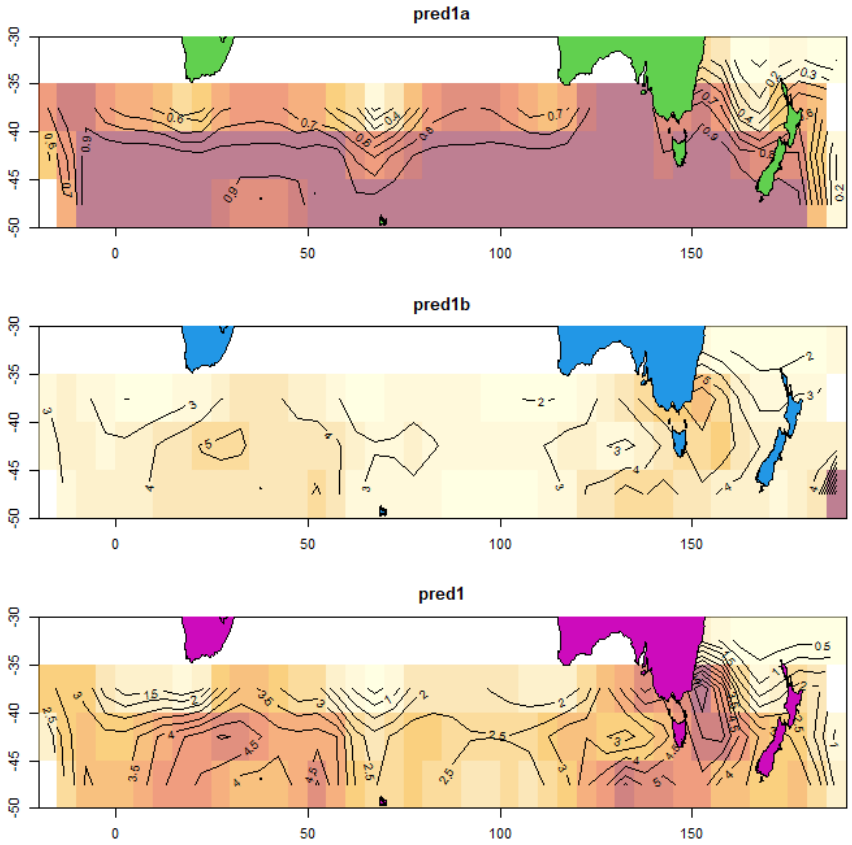


Fig. 18. Predicted value on map in the base case run.
See Fig. 14.

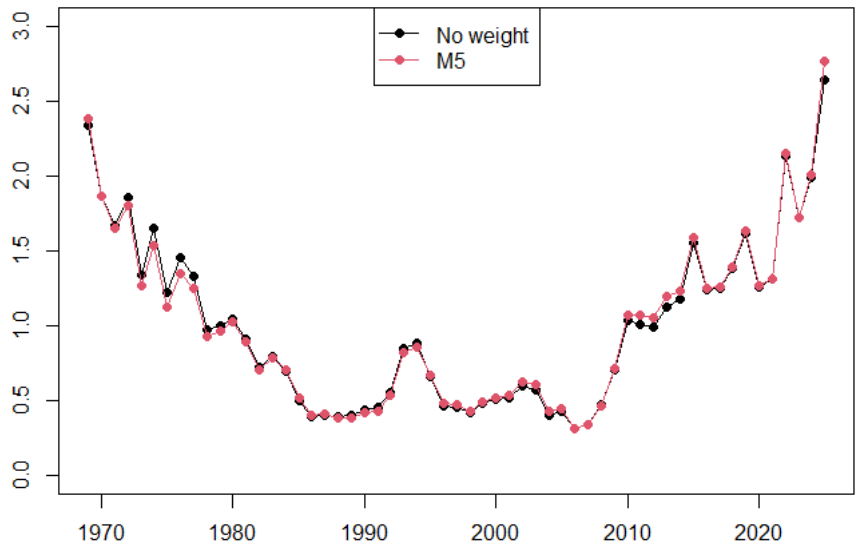


Fig. 19. Comparison of area weighted abundance indices in the base case run.
Red (M5) is area weighted abundance index of GAM22 which take into account that the longitude length changes over latitude and the number of 1x1 degree squares ever fished in a 5x5 degrees square. Black is the abundance index which weighting was not considered.

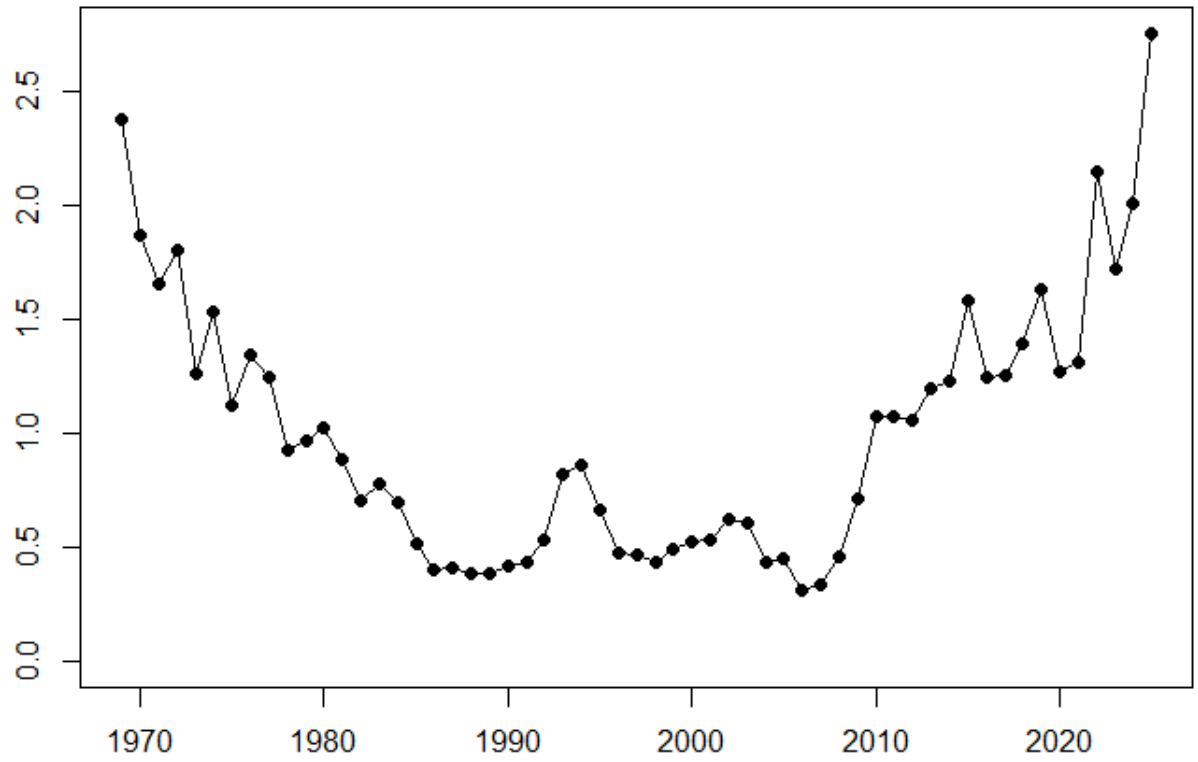


Fig. 20. CPUE abundance index for the base case.

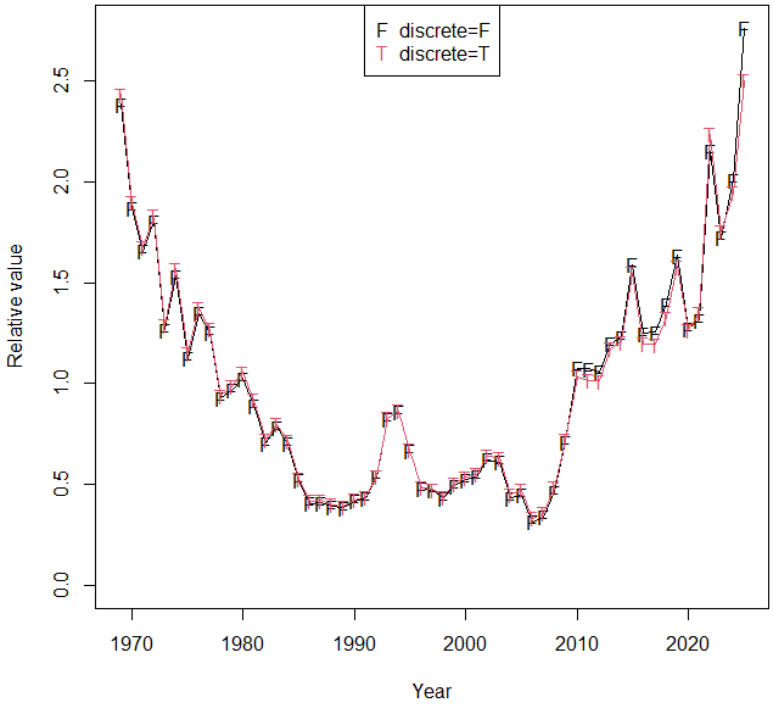


Fig. 21. CPUE abundance index for the base case of original (discrete=F) and referred to in the sensitivity analysis (discrete=T).

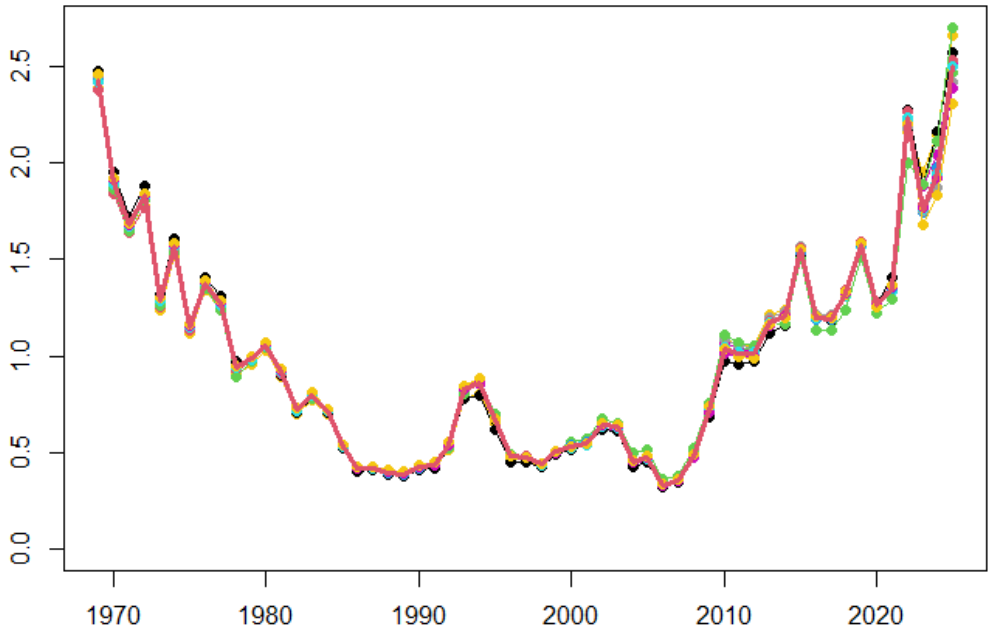


Fig. 22. Sensitivity analysis of model selection in the binomial sub-model for all runs.

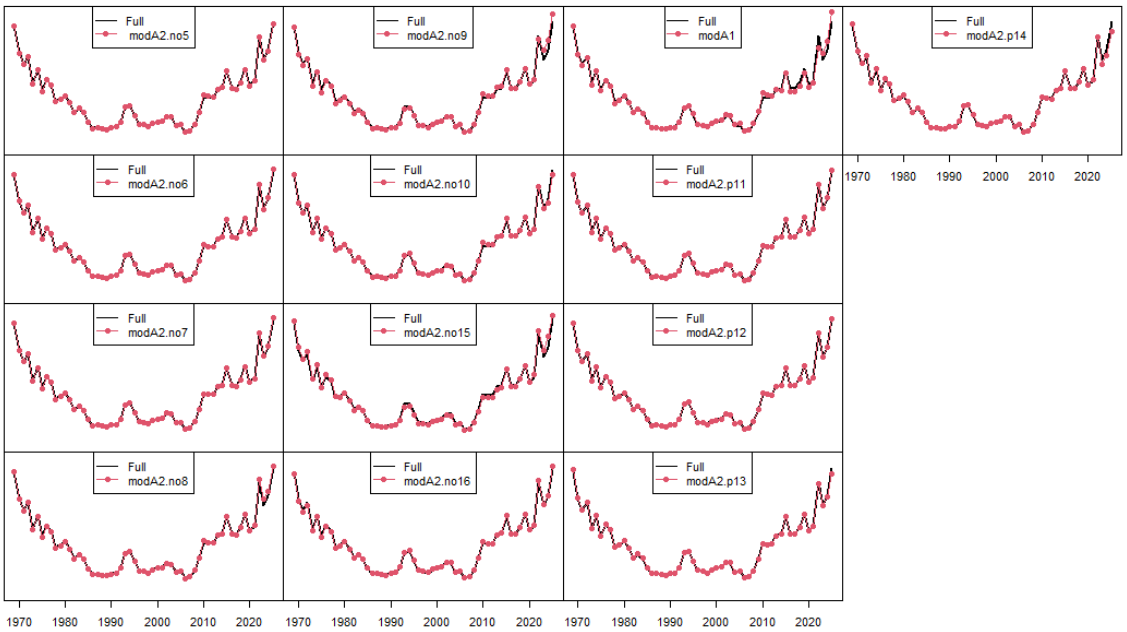


Fig. 23. Sensitivity analysis of model selection in the binomial sub-model for each run.
Full represents modA2.

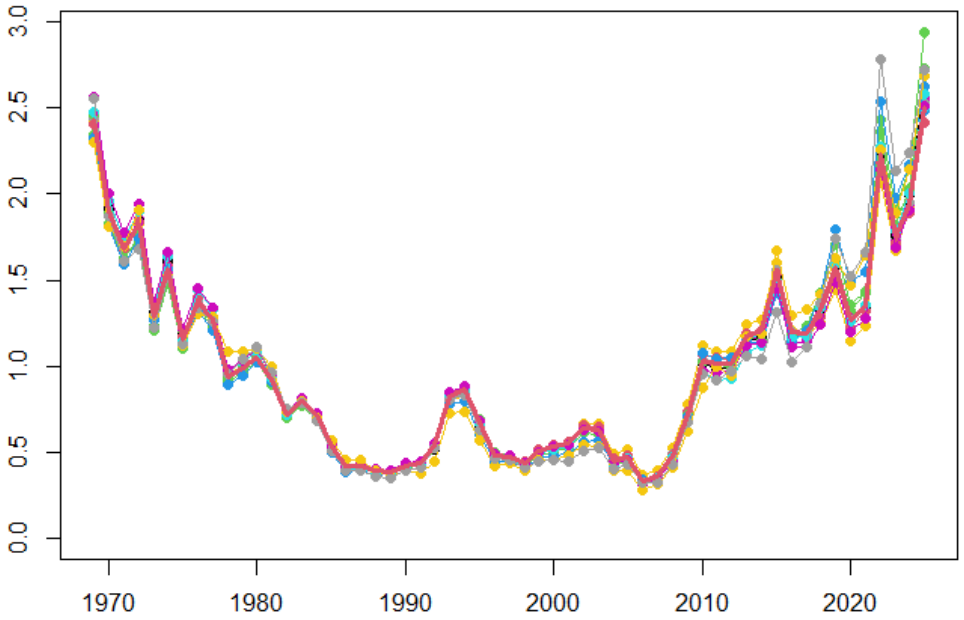


Fig. 24. Sensitivity analysis of model selection in the positive catch sub-model for all runs.

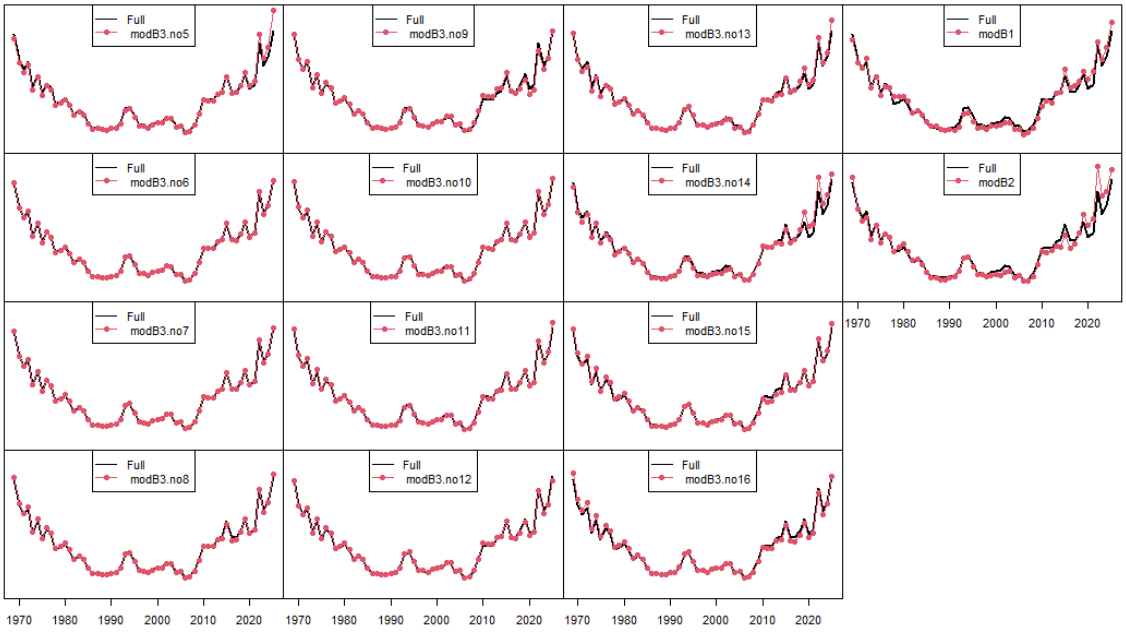


Fig. 25. Sensitivity analysis of model selection in the positive catch sub-model for each run.
Full represents modB3.

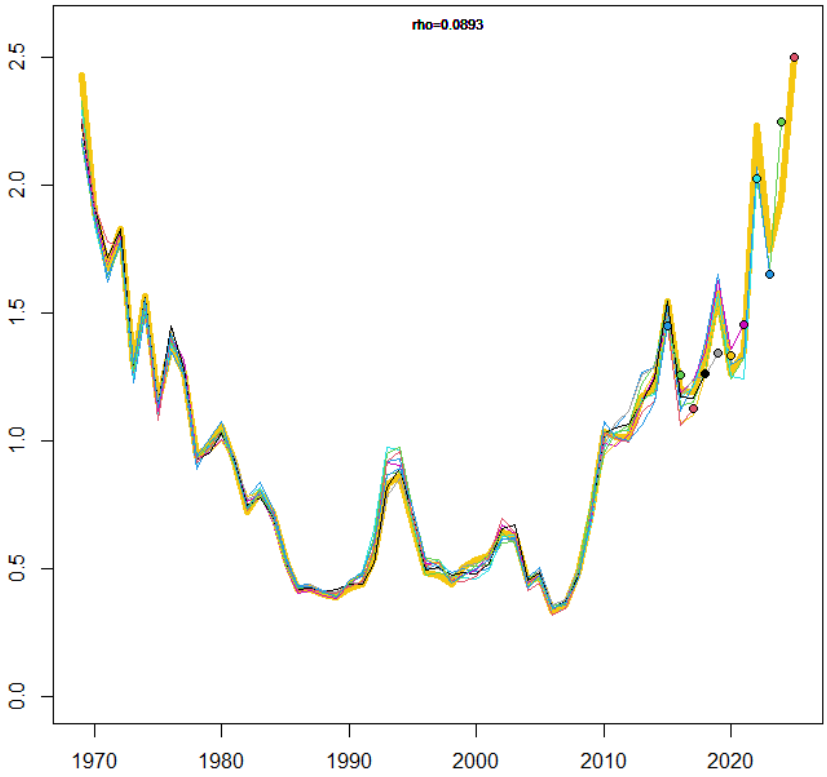


Fig. 26. Retrospective analysis for the base case model.
Rho represents Mohn's rho.

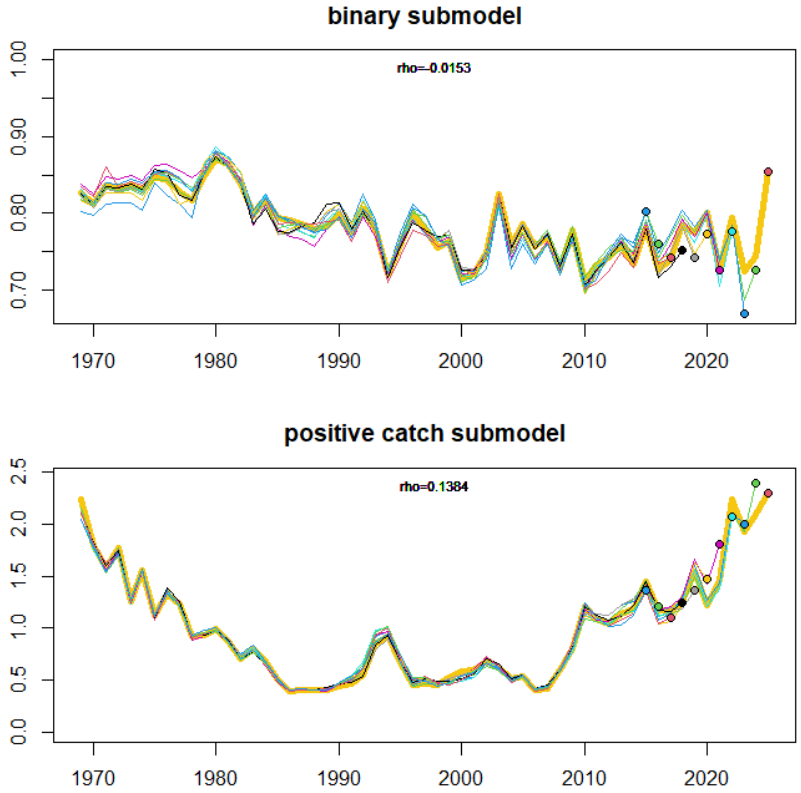


Fig. 27. Retrospective analysis for the base case model by sub-model.
Upper panel is by binomial submodel, and lower panel is by positive catch submodel. Rho represents Mohn's rho.

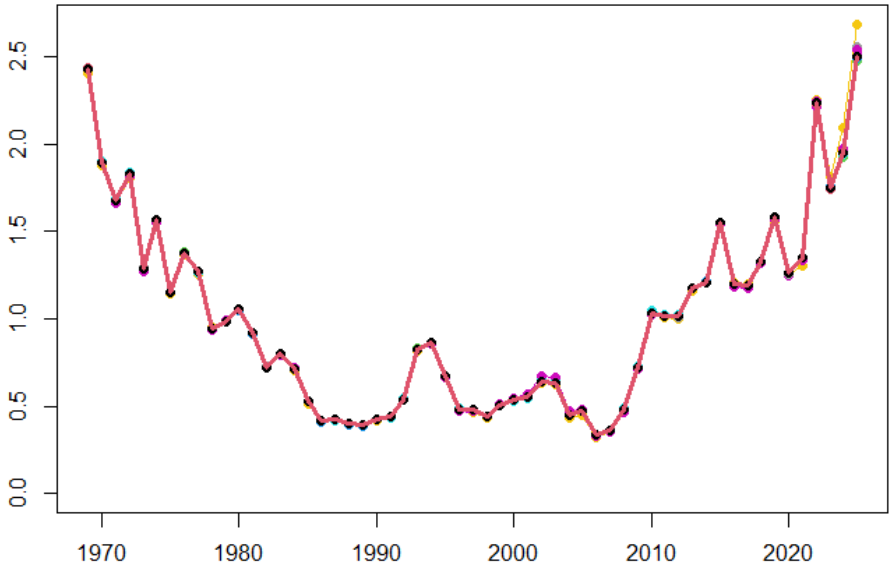


Fig. 28. Sensitivity analysis of k-value in the binomial sub-model for all runs.

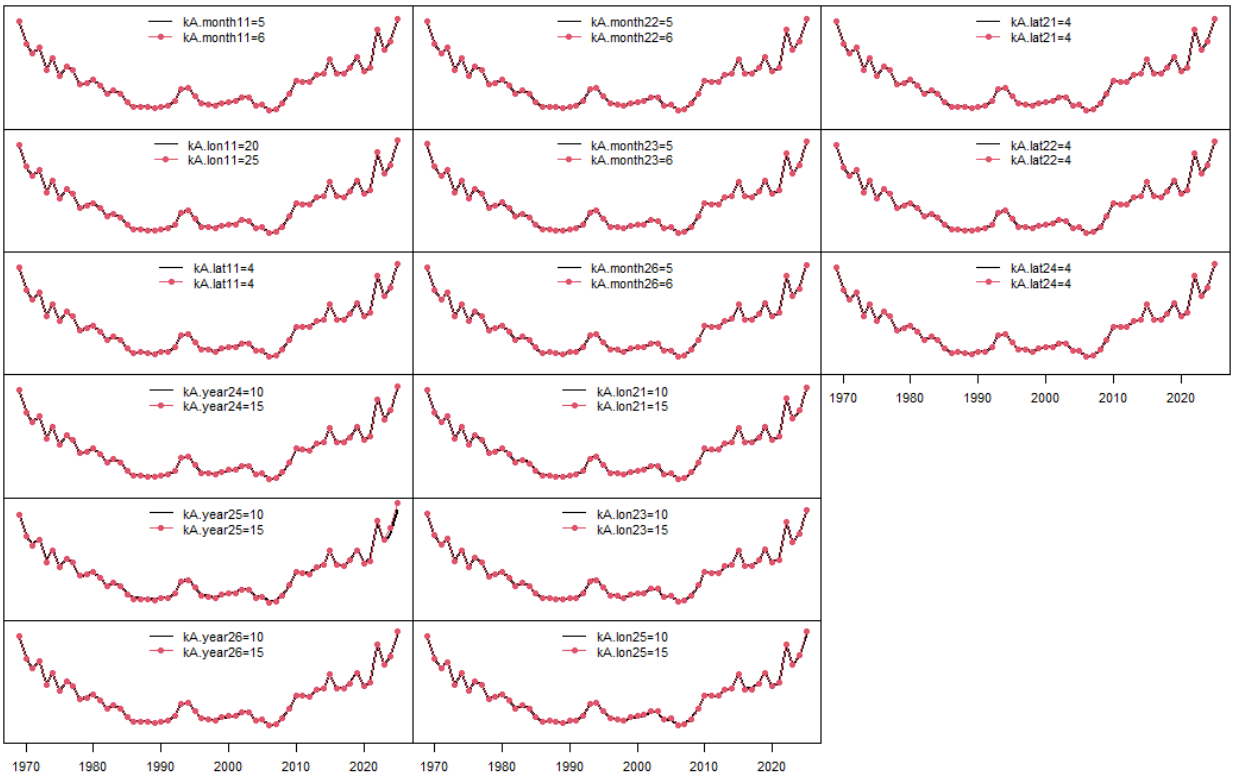


Fig. 29. Sensitivity analysis of k-value in the binomial sub-model for each of run.

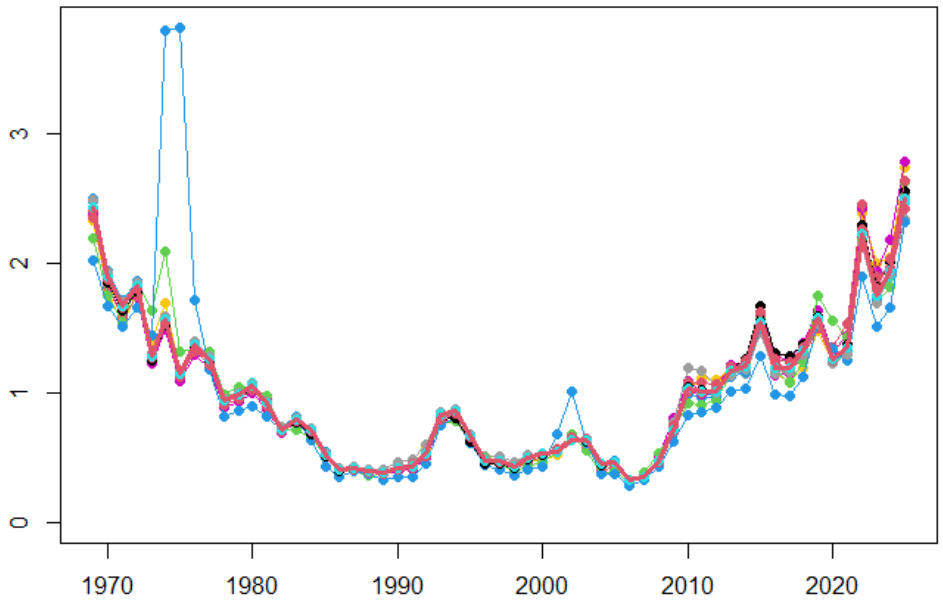


Fig. 30. Sensitivity analysis of k-value in the positive catch sub-model for all runs.

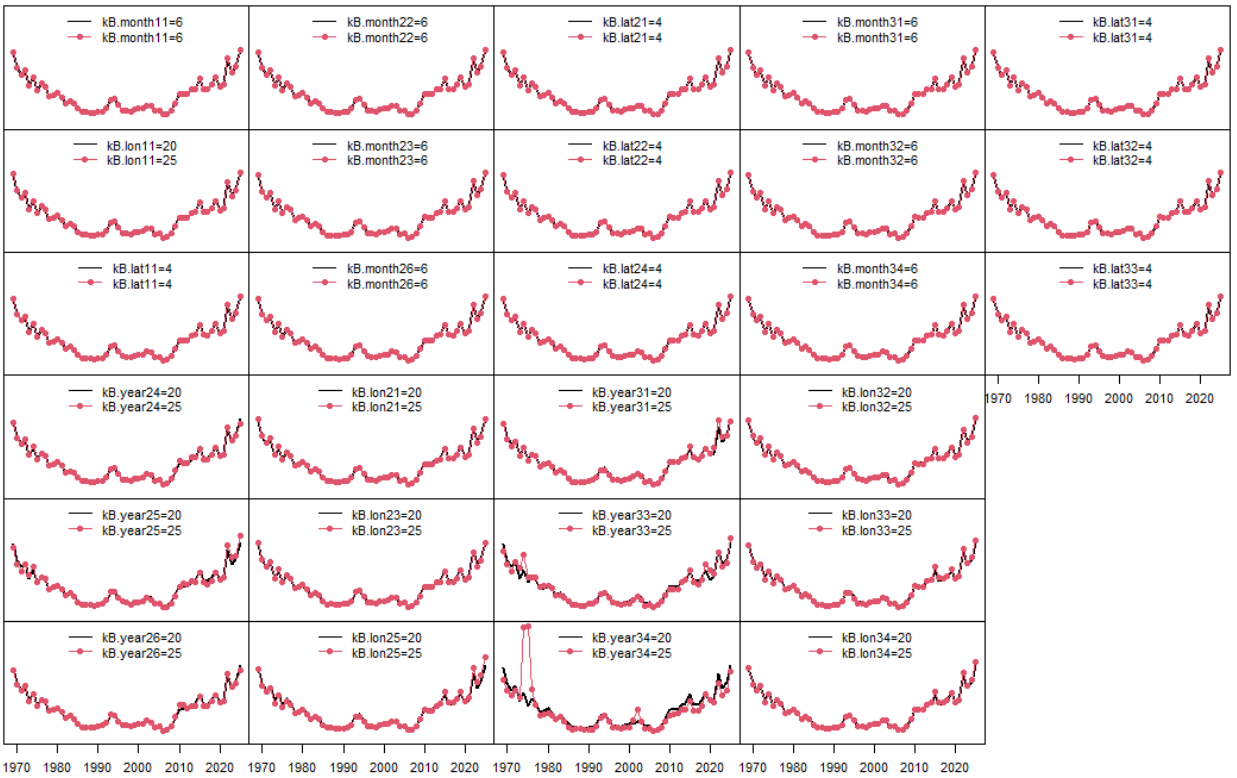


Fig. 31. Sensitivity analysis of k-value in the positive catch sub-model for each of run.

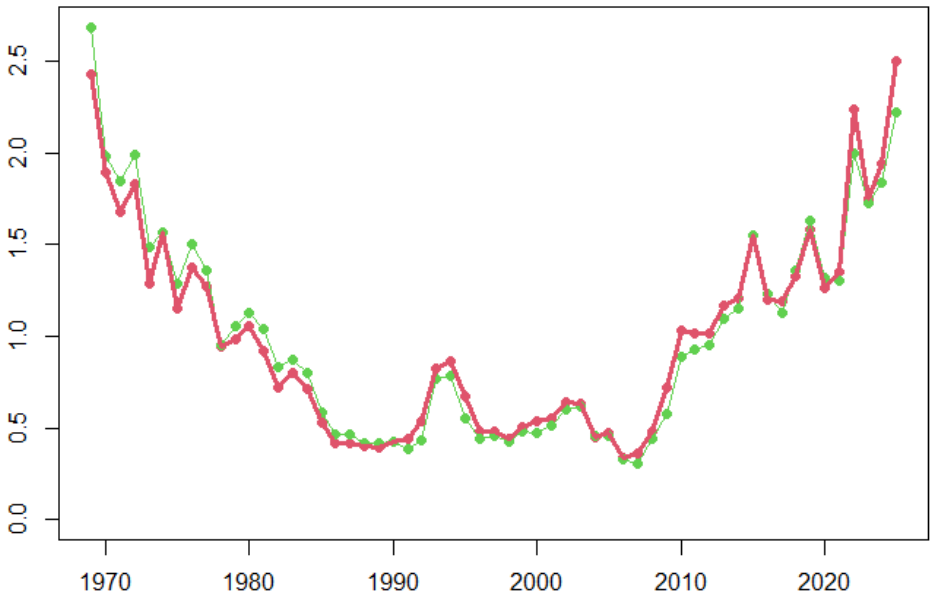


Fig. 32. Sensitivity analysis for the effect of age-5 plus instead of age-4 plus.
Red is the base case, and green is the sensitivity run (age-5 plus).

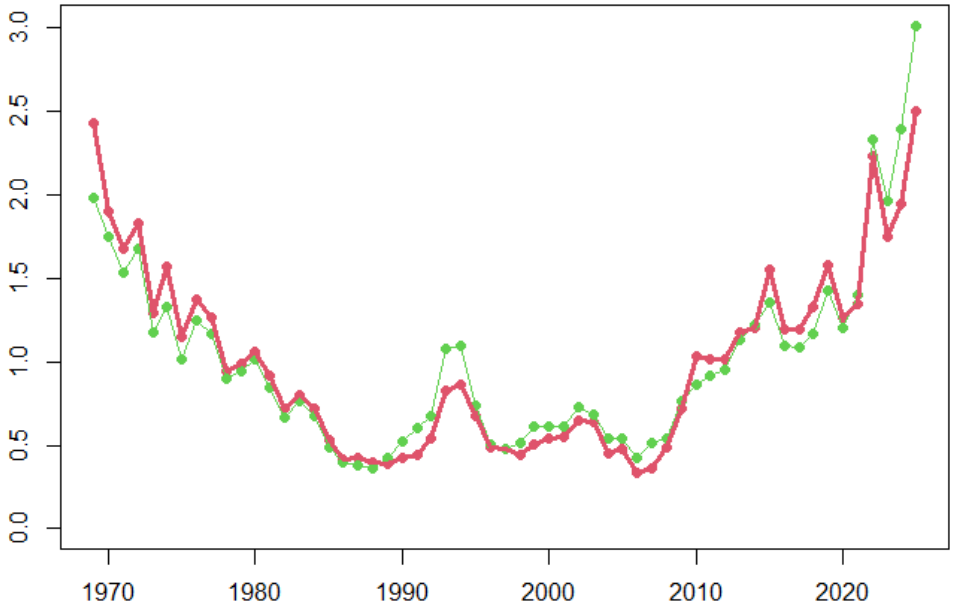


Fig. 33. Sensitivity analysis for the effect of all ages instead of age-4 plus.
Red is the base case, and green is the sensitivity run (all ages).

Table 1. The k values selected for each of sub-model.

Submodel	BSM	PCSM
k.month11	5	6
k.lon11	20	20
k.lat11	4	4
k.year24	10	20
k.year25	10	20
k.year26	10	20
k.month22	5	6
k.month23	5	6
k.month26	5	6
k.lon21	10	20
k.lon23	10	20
k.lon25	10	20
k.lat21	4	4
k.lat22	4	4
k.lat24	4	4
k.year31		20
k.year33		20
k.year34		20
k.month31		6
k.month32		6
k.month34		6
k.lon32		20
k.lon33		20
k.lon34		20
k.lat31		4
k.lat32		4
k.lat33		4

Table 2. Statistics of choosing k values in the two sub-models of GAM.

BSM

Term	k'	edf	k-index	p-value
ti(month)	4	3.26	0.9743	0.07
ti(lon.cnt)	19	18.53	0.9837	0.20
ti(lat)	3	1.32	0.9775	0.11
ti(lon.cnt,lat)	27	23.78	0.9939	0.50
ti(month,lat)	12	8.34	0.9615	0.07
ti(lon.cnt,month)	36	31.93	0.9838	0.31
ti(year,lat)	27	22.52	0.9738	0.26
ti(year,lon.cnt)	81	72.52	1.0196	0.89
ti(year,month)	36	33.15	1.0156	0.81
s(log(hook))	9	7.62	0.9909	0.40

PCSM

Term	k'	edf	k-index	p-value
ti(month)	5	4.74	1.0079	0.71
ti(lon.cnt)	19	17.16	0.9959	0.34
ti(lat)	3	2.66	1.0153	0.87
ti(lon.cnt,lat)	57	29.19	1.0024	0.55
ti(month,lat)	15	7.63	0.9903	0.23
ti(lon.cnt,month)	95	64.54	0.9980	0.45
ti(year,lat)	57	21.30	0.9929	0.31
ti(year,lon.cnt)	361	189.06	0.9911	0.21
ti(year,month)	95	41.46	0.9785	0.05
ti(lat,month,year)	285	125.29	0.9302	0.00
ti(lat,lon.cnt,month)	285	76.10	0.9481	0.00
ti(lat,lon.cnt,year)	1083	353.36	0.9634	0.01
ti(year,lon.cnt,month)	1805	784.87	0.9541	0.00
s(log(hook))	9	7.58	1.0172	0.85

Table 3. Diagnostic statistics of GAM.

Sub-model	BSM	PCSM
n.data	811,642	715,383
dev.expl	73.83%	49.79%
AIC	155,282	1,517,576
residual.df	811,359	713,598
REMLscore	412,480	382,577

Table 4. Abundance index of GAM22 as the base case.

Year	Index
1969	2.38372
1970	1.86932
1971	1.65577
1972	1.80291
1973	1.26648
1974	1.53344
1975	1.12525
1976	1.34921
1977	1.25144
1978	0.92998
1979	0.96884
1980	1.02587
1981	0.89175
1982	0.70659
1983	0.78391
1984	0.70347
1985	0.52037
1986	0.40728
1987	0.41030
1988	0.39070
1989	0.38541
1990	0.41898
1991	0.43465
1992	0.53897
1993	0.82636
1994	0.86150
1995	0.66966
1996	0.48218
1997	0.47402
1998	0.43423
1999	0.49514
2000	0.52470

Year	Index
2001	0.53840
2002	0.62475
2003	0.61177
2004	0.43423
2005	0.45052
2006	0.31695
2007	0.33945
2008	0.46327
2009	0.71269
2010	1.07521
2011	1.07495
2012	1.05855
2013	1.19784
2014	1.22980
2015	1.58897
2016	1.24723
2017	1.25589
2018	1.39316
2019	1.63346
2020	1.27245
2021	1.31528
2022	2.15071
2023	1.72294
2024	2.00857
2025	2.76059

Table 5. Results of sensitivity analysis for model selection in the binomial sub-model.

name	term	dev.expl	AIC	residual.df	REMLscore	dAIC
modA2	Main and 2 way interactions	73.83%	155,282	811,359	412,480	2,603
modA2.no5	-ti(lon, lat)	73.25%	158,619	811,381	413,187	5,940
modA2.no6	-ti(month, lat)	73.59%	156,693	811,367	412,826	4,014
modA2.no7	-ti(lon, month)	73.48%	157,263	811,390	412,918	4,584
modA2.no8	-ti(year, lat)	73.16%	159,188	811,379	413,432	6,509
modA2.no9	-ti(year, lon)	72.54%	162,714	811,431	414,172	10,035
modA2.no10	-ti(year, month)	72.90%	160,704	811,391	413,771	8,025
modA2.no15	-cl	71.12%	171,277	811,358	416,518	18,598
modA2.no16	-s(log(hook))	73.48%	157,342	811,366	412,994	4,663
modA1	Main effects	67.40%	192,882	811,548	421,384	40,203
modA2.p11	+ti(lat, month, year)	74.24%	152,877	811,334	411,919	198
modA2.p12	+ti(lat, lon, month)	74.09%	153,785	811,329	412,219	1,106
modA2.p13	+ti(lat, lon, year)	74.06%	153,994	811,329	412,262	1,315
modA2.p14	+ti(year, lon, month)	74.29%	152,679	811,308	411,934	0

Table 6. Results of sensitivity analysis for model selection in the positive catch sub-model.

name	term	dev.expl	AIC	residual.df	REMLscore	dAIC
modB3	Full model	49.78%	1,517,693	713,618	382,588	14
modB3.no5	-ti(lon, lat)	49.78%	1,517,712	713,610	382,628	33
modB3.no6	-ti(month, lat)	49.78%	1,517,689	713,617	382,593	10
modB3.no7	-ti(lon, month)	49.78%	1,517,679	713,606	382,616	0
modB3.no8	-ti(year, lat)	49.78%	1,517,747	713,614	382,608	67
modB3.no9	-ti(year, lon)	49.76%	1,517,950	713,618	382,661	271
modB3.no10	-ti(year, month)	49.78%	1,517,716	713,620	382,593	37
modB3.no11	-ti(lat, month, year)	49.70%	1,518,671	713,707	382,716	992
modB3.no12	-ti(lat, lon, month)	49.71%	1,518,564	713,656	382,780	885
modB3.no13	-ti(lat, lon, year)	49.41%	1,522,531	713,835	383,525	4,851
modB3.no14	-ti(year, lon, month)	48.67%	1,532,117	714,219	385,369	14,438
modB3.no15	-cl	49.49%	1,521,786	713,611	383,628	4,107
modB3.no16	-s(log(hook))	49.74%	1,518,257	713,613	382,735	577
modB1	Main effects	41.49%	1,623,672	715,288	406,273	105,993
modB2	Main and 2 way interactions	47.50%	1,547,190	714,745	388,367	29,510